ROCK inhibitor Y-27632 maintains the proliferation of confluent human mesenchymal stem cells

Kouhei Nakamura, Atsutoshi Yoshimura, Takashi Kaneko, Kayo Sato, Yoshitaka Hara

Department of Periodontology, Nagasaki University Graduate School of Biomedical Sciences, Nagasaki University, Nagasaki, Japan

Running title: Y-27632 maintains confluent MSC growth

Corresponding author: Yoshitaka Hara, 1-7-1 Sakamoto, Nagasaki 852-8588, Japan; Tel: +81-95-819-7683; Fax: +81-95-819-7684; E-mail address: harasen@nagasaki-u.ac.jp

Keywords: mesenchymal stem cells (MSCs), cell proliferation, ROCK inhibitor, cell-sheets

Abstract

Background and Objective: The transplantation of cell-sheets of mesenchymal stem cells (MSCs) is expected to be the next generation of periodontal regenerative therapy. An adequate method of multi-layering MSCs has yet to be established. When cell-sheets proliferate, they usually contract and detach from culture dishes and then the proliferation of cells in the contracted areas is arrested. ROCK-mediated contractile force causes cell contraction. Although multilayer formation medium (MFM) stimulated the proliferation of growth-arrested confluent MSCs, MSCs detached from culture dish. Therefore, we investigated the effects of ROCK inhibitor Y-27632 on the proliferation and detachment of confluent MSCs, and examined the ability of differentiation of the cells contained in the cell-sheets.

Materials and Methods: Confluent MSCs were cultured in MFM containing transforming growth factor-β1, ascorbic acid, and fetal bovine serum either with or without Y-27632. Cell proliferation was examined by BrdU incorporation assays and total DNA measurement. Sheet contractions were examined by light microscopy and stereomicroscopy. Multilayer formations and focal adhesion assembly were observed with confocal microscopy. Characteristic of cells were examined by flow cytometric

analysis. Osteoblast lineage differentiation was observed with ALP and alizarin red S staining. Adipocyte lineage differentiation was observed with oil red O staining.

Results: The addition of Y-27632 to MFM prevented the cell-sheets from detaching and did not inhibit MSC growth. The cell numbers cultured with MFM/Y-27632 were significantly higher than that obtained with MFM-only on day-4. Cell-sheets detached from the culture dish on day-4, and the number of BrdU-positive cells in the detached area decreased. The cells in the cell-sheets were similar characteristic to primary MSCs, and differentiated into osteoblast and adipocyte lineages.

Conclusion: Y-27632 both prevented the MSC-sheets from detaching and maintained the multilayered proliferation of confluent MSCs by MFM, and then cells in the sheets had differentiation potency.

Introduction

Periodontal tissue regeneration is a major goal of periodontal therapy. However, therapeutical methods of periodontics have not yet achieved perfect periodontal regeneration with the re-formation of all components of the periodontal ligament. Transplantation of mesenchymal stem cells (MSCs) is expected to be the next generation of periodontal regenerative therapy (1). The success rate of transplantation of MSCs increases with an increase in the numbers of MSCs used (2, 3), and cell-sheets have been found to provide more advantages than injections of cell suspensions (4). For the creation of MSC-sheets, a method of multi-layering MSCs is required, and several groups have used multilayered MSC-sheets cultured with osteoblastic differentiation medium (5–7). However, MSCs with multilineage potential are thought to be beneficial for the regeneration of periodontal ligament, in which several types of cells are present.

In routine culture, normal fibroblasts stop dividing as they grow to confluence, a phenomenon known as density-dependent inhibition of growth. Treatment of confluent fibroblasts with transforming growth factor-β1 (TGF-β1), in the presence of ascorbic acid and serum, stimulates proliferation, leading to cell stratification (8). We improved this medium, produced multilayered fibroblast-sheets, and named the medium multilayer formation medium (MFM) (9). However, there is little knowledge about the

effects of MFM on MSCs. In preliminary experiments, we cultured MSCs with MFM. Though MFM consisting of TGF-β1, L-ascorbic acid 2-phosphate (AsAP: a stable form of ascorbic acid) and fetal bovine serum (FBS) stimulated the proliferation of growth-arrested confluent MSCs, the detachment of cell-sheets was observed on day-3 or 4 (data not shown).

TGF-β1 activates ROCK (or Rho kinase) (10) and is thought to generate ROCK-dependent actomyosin contractile forces (11, 12). At the same time, focal adhesion is then formed simultaneously (13, 14). Contractile force detaches cell-sheets from conventional tissue culture dishes (15). The detachment of cell-sheets decreases their metabolic activity, and the growth of the cells in the sheets goes into arrest (16). These unexpected phenomena of multilayered MSCs are still unsolved. We hypothesized that adjustment of the force generation is important to produce high-cell-density MSC-sheets. Y-27632, which is known as a highly selective ROCK inhibitor (17, 18), releases cell contractions (19) and maintains the pluripotency of stem cells (20). In preliminary experiments, Y-27632 did not prevent confluent MSC growth by MFM (data not shown). Therefore, we examined the Y-27632 effects of the detachment of cell-sheets, which was accompanied by MSC multilayer growth, and the differentiation potential of the cells contained in the sheets.

Materials and Methods

Cells

Human bone marrow-derived MSCs were purchased from Lonza (Walkersville, MD, USA). The cells were positive for the expression of CD29, CD44, CD105, and CD166, negative for the expression of CD14, CD34, and CD45, and capable of differentiating into osteoblasts, chondrocytes, and adipocytes (according to the manufacturer's instructions). The cells were used at early passage (passage two or three), and they were grown in α-minimal essential medium (α-MEM) (Gibco BRL, Grand Island, NY, USA) supplemented with 10% FBS and antibiotics (100 U/mL penicillin and 100 μg/mL streptomycin). All cultures were maintained in a humidified atmosphere of 95% air and 5% CO_2 at 37°C.

Experimental conditions

Cells were seeded on human plasma fibronectin-coated 24- or 96-well tissue culture plates (Falcon; Becton Dickinson, Lincoln Park, NY, USA) or 4-well Lab-Tek II chamber glass slides (Nunc, Naperville, IL, USA) at subconfluence (5×10^3 cells/cm^2) and allowed to grow to confluence in α-MEM containing 10% FBS and antibiotics within 8–10 days. The day of confluence was set as day 0. The proliferation of confluent cells was stimulated with MFM either with or without the ROCK inhibitor Y-27632

(10 μM; Merck KGaA, Darmstadt, Germany). The MFM consisted of S-Clone medium (EIDIA, Tokyo, Japan) containing human plasma TGF-β1 (1 ng/mL; R&D Systems, Minneapolis, MN, USA), AsAP (0.15 mM; Wako Pure Chemical Industries, Osaka, Japan), 10% FBS, and antibiotics, as described (9). Concentration of Y-27632 was determined as follows. Y-27632 was used at 10 μM according to our previous study of fibroblasts (9) and other groups' experiments (20, 21), and when we used Y-27632 at 0.1, 1, 5 and 10 μM, there was no difference in the percentage of BrdU-positive cells in 2-day BrdU incorporation assays. The S-Clone is a combined medium of slightly modified RPMI 1640, DMEM, and Ham's F12 and contains the following supplements: insulin, transferrin, selenium, 0.1% bovine albumin, ethanolamine, mercaptoethanol, sodium bicarbonate, and HEPES (manufacturer's instructions). The medium (including test factors) was changed every 2 days.

Assay of the areas of the MSC-sheets

Cells in 24-well plates were fixed with 1% paraformaldehyde in 0.1 M cacodylate buffer (pH 7.4) containing 5% sucrose for 30 min and washed with PBS. Each MSC-sheet was stained with Coomassie brilliant blue R-250 (Nacalai Tesque, Kyoto, Japan) for 30 min and washed with PBS. The images were taken with a digital camera and stereomicroscope (Leica MZ16 F, Leica Microsystems, Wetzlar, Germany).

The proportion of surface area of cell-sheets was determined by processing the images in Adobe Photoshop (22). Briefly, we traced the edge of the cell-sheets and wells by means of the Lasso tool of Adobe Photoshop, selected defined tracing areas of sheets and wells, measured the pixel numbers of each area, and calculated the area ratio.

Assays for cell number and proliferation

DNA was purified from MSCs with the QIAamp DNA Mini Kit (Qiagen, Germantown, MD, USA) and measured with a spectrophotometer (NanoDrop 1000, NanoDrop Products, Wilmington, DE, USA). For the evaluation of cell viability, cells were incubated with neutral red (33 mg/mL; Gibco BRL) for 1 h at 37°C, fixed with 1% paraformaldehyde for 30 min, and observed by light microscopy (23). DNA-synthesizing cells, as an indicator of proliferative capacity, were detected by a bromodeoxyuridine (BrdU) incorporation assay, as described (9). Briefly, cells in 24-well plates were labeled with 50 μM BrdU (Sigma, St. Louis, MO, USA) during the last 20 h of incubation. The cells were fixed with 1% paraformaldehyde in 0.1 M cacodylate buffer (pH 7.4) containing 5% sucrose for 30 min, and then washed with PBS. Subsequently, the cells were permeabilized with buffered formalin acetone for 1 min, treated with 2 N HCl for 20 min to denature DNA, and rinsed with 0.1 M borate buffer (pH 8.5) for 2 min. Immunostaining with anti-BrdU mAb (Bu20a; 1:50 dilution;

DakoCytomation, Glostrup, Denmark) was performed using a Vectastain Universal Quick kit (Vector, Burlingame, CA, USA). Peroxidase activity was visualized with 3.3′-diaminobenzidine tetrahydrochloride and H_2O_2. The nuclei were counterstained with hematoxylin. The numbers of total and BrdU-positive cells were counted on light micrographs taken from ten randomly selected fields (0.4 mm^2/field) of each well. The percentage of BrdU-positive cells and the cell density (cell numbers/field) were determined by examining at least 1,500 cells/well.

Immunofluorescence

Cells in Lab-Tek II chamber glass slides were fixed with 1% paraformaldehyde in 0.1 M cacodylate buffer (pH 7.4) containing 5% sucrose for 30 min, washed with PBS, and permeabilized with 0.5% Triton X-100 for 5 min. The cells were then washed with PBS and blocked with 3% BSA for 30 min. The primary antibodies used were mouse anti-paxillin mAb 349 (1:100 dilution; BD Biosciences, San Jose, CA, USA) and mouse anti-vinculin mAb HVIN-1 (1:100 dilution; Sigma). The cells were incubated with the primary antibodies for 1 h, followed by incubation with Alexa Fluor 488-labeled donkey anti-mouse IgGs (Molecular Probes, Eugene, OR, USA). Immunostaining specificity was checked by replacing the primary antibody with normal mouse IgG, and no fluorescence was found in the controls. Cell nuclei were visualized

with TO-PRO-3 iodide (642/661) (Molecular Probes). Coverslips were mounted onto slides using SlowFade Gold antifade reagent (Molecular Probes). Confocal images were obtained with a Zeiss LSM 510 META laser scanning microscopy system (software ZEN 2008; Carl Zeiss MicroImaging, Jena, Germany). The images were adjusted with the Level function in Adobe Photoshop to remove the background. We gave careful consideration to the localization of cell nuclei and molecules at sites of cell-substrate and cell-cell contacts by examining a *z*-axis series of confocal images captured from the base to the top plane of cells, as described (9). The cross-sectional image was obtained by computer processing of stacked images.

Flow Cytometric Analysis

The primary MSCs purchased from Lonza and the cultured cells forming cell-sheets were performed by flow cytometric analysis. Briefly, 20000-100000 cells were stained with primary antibody: mouse anti-human mAb CD90, CD105, CD146, CD166, CD44, CD19 and CD45, secondly antibody goat anti-mouse phycoerythrin (R&D Systems). Selection of antibodies was referring to previous reports (24, 25). Cells were analyzed by flow cytometry (FACSCanto II, BD Biosciences). Data were analyzed using FlowJo software (Tree Star, Ashland, OR, USA).

Differentiation potential assay

To confirm differentiation potential, cells from multilayered cell-sheets were cultured with osteogenic and adipogenic induction medium (Lonza) according to the manufacturer's instructions. Briefly, cell cultures with MFM/Y-27632 (MFM/Y) for 4 days were detached with 0.05% Trypsin/EDTA and suspended in α-MEM containing 10% FBS. Cells were plated in 24-well plate at 5×10^3 cells/cm^2, allowing the cells to adhere to the culture surface for 24 h in α-MEM containing 10% FBS. To induce osteogenic differentiation, medium was replaced with osteogenic induction medium and cells were cultured for further 21 days. The control cells were cultured with α-MEM containing 10% FBS. Osteogenic differentiation was demonstrated by alkaline phosphatase (ALP) and alizarin red S staining. For ALP staining on day-4, the cells were washed once with sterilized PBS, followed with the standard protocol of ALP staining kit (TaKaRa Bio, Shiga, Japan). Briefly, the cells were fixed in 150 mL of fixation solution for 5 min and washed twice with sterilized distilled water, stained with 100 mL of ALP substrate solution, and incubated at 37°C for 15 to 45 min. The period for ALP color formation varied depending on the amount of phosphates present in the cells. For alizarin red S staining on day-21, the cells were washed once with sterilized PBS, fixed in methanol, and stained with calcified nodule staining kit (Primary Cell, Hokkaido, Japan). To induce adipogenic differentiation, adipogenic induction and

maintenance media were used alternately every 3 days for 18 days. The control cells were cultured only with adipogenic maintenance medium. The presence of intracellular lipid vesicles visible was assessed by oil red O staining. Briefly, cells in 24-well plates were fixed with 1% paraformaldehyde in 0.1 M cacodylate buffer (pH 7.4) containing 5% sucrose for 15 min and washed with PBS. The cells were stained with oil red O (Primary Cell) for 30 min and washed with PBS.

Statistics

Each experiment was performed three times and each was assayed in duplicate or triplicate wells. Data are presented as means ± SD. Statistical analyses were performed by one-way analysis of variance (ANOVA) followed by Tukey's *post hoc* test.

Results

Confluent MSCs which were exposed to MFM for 3 or 4 days contracted and detached from the culture wells at the periphery of the cell-sheets. This resulted in a decrease in the surface area of the cell-sheets to 63 ± 5.7% of the original area on day 4 ($p = 0.0004$) (Fig. 1A,B). In contrast, neither contraction of cell-sheets nor a reduction in their surface area was observed after a 4-day incubation with MFM/Y (Fig. 1A,B). This experiment was performed three times and was assayed in duplicate wells (a total of 6 wells). The cell numbers in both areas were counted by measuring total DNA in time-course studies for up to 4 days. The numbers of cells in the cultures with MFM/Y were similar to those obtained with MFM on day 2 (MFM/Y, 5.9 ± 0.8, MFM, 5.2 ± 1.1; $p = 0.39$) and were significantly higher than those obtained with MFM on day 4 (MFM/Y, 13.1 ± 1.4, MFM, 9.6 ± 1.2; $p = 0.009$) (Fig. 1C). These results suggest that sheet contraction influenced the proliferation of the cells forming the cell-sheet. Similar results were obtained in three independent experiments.

To explore the cause of difference in number of cells on day-4, we investigated the proliferative capacity of the contracted and detached areas. The contracted area of the cell-sheets cultured with MFM for 4 days displayed no BrdU-labeling; however, the attached area without contraction contained several BrdU-positive cells under

light-microscopic observation (Fig. 2A,B). We refer to the former and latter as the area of contraction (CT) and non-contraction (non-CT), respectively, and both areas were well distinguishable (Fig. 2A,B). There were no cells in the detached area (Fig. 2C). BrdU-labeled cells were distributed throughout the cell-sheets cultured with MFM/Y (Fig. 2D). Cells in the non-CT areas were spindle-shaped and densely arranged in a circular pattern (data not shown), whereas those in the CT areas were elongated and aggregated parallel to the edge (Fig. 2E). The cells in each condition were stained with neutral red, indicating cell viability (data not shown).

We compared the non-CT areas cultured with MFM (MFM non-CT) to the cell-sheets cultured with MFM/Y. We performed immunofluorescence staining and examined the results with confocal microscopy. Couple of overlapping nuclei was observed in cross-sectional images of the cell-sheets cultured with both MFM and MFM/Y for 4 days (Fig. 3A). There was no significant difference in the cell density and the proportion of BrdU-positive cells between the MFM non-CT and the cell-sheets cultured with MFM/Y for 4 days (Cell density, MFM non-CT, 398.3 ± 10.2, MFM/Y, 411.0 ± 19.3; $p = 0.37$) (BrdU-labeled cells, MFM non-CT, 19.4 ± 5.0%, MFM/Y, 25.4 ± 4.8%; $p = 0.20$) (Fig. 3B,C).

To investigate the focal adhesion assembly, we examined paxillin or vinculin, a

component of focal adhesions (26). In a *z*-axis series of confocal images, paxillin was not localized at the base of cells cultured with FBS alone (Fig. 4). The culture with MFM showed paxillin at the base of cells (Fig. 4). In contrast, when Y-27632 was added to the MFM, paxillin was not observed at the base of cells (Fig. 4). There was no difference in the number of cell nuclei between the three conditions (Fig. 4). The localization pattern of vinculin in three types of culture medium was similar to those of paxillin (data not shown).

In order to compare the characteristics of the primary MSCs purchased from Lonza and the cultured cells forming cell-sheets, we performed flow cytometric analysis and differentiation potential assay. The analysis of surface markers indicated that the primary cells and the cells of sheets have a very similar immunophenotype (Fig. 5). In differentiation experiments, cells containing our cell-sheets were cultured with osteogenic or adipogenic induction medium (Fig. 6A–E). In the osteogenic differentiation experiments, the cells changed their morphology from spindle shaped to cuboidal and experimental group was induced ALP activity compared with control group on day-4 (Fig. 6A,B). On day-21, alizarin red S staining indicated calcium deposition (Fig. 6C). The cells in control were detached from culture dish surface and not stained. In the adipogenic differentiation experiments, the accumulation of lipid

vacuoles was microscopically observed in the cells, however, not in the control (Fig. 6D,E).

Discussion

In the preliminary experiments, MFM consisting of TGF-β1, AsAP and FBS stimulated the proliferation of growth-arrested confluent MSCs. In the BrdU incorporation assays, MFM was more potent for the proliferation of confluent MSCs than the culture media lacking any one or two of TGF-β1, AsAP, and FBS (data not shown). On the other hand contractile force enhanced the contraction of cells and the detachment of cell-sheets (15) when TGF-β1 stimulated the proliferation of confluent cells. Detached cell-sheets are thought to decrease their metabolic activity and go into growth arrest (16). In the present study, about 40% of the marginal region of cell-sheets detached from the culture wells, and the numbers of BrdU-labeled cells in the CT areas were clearly less than those in the non-CT areas cultured with MFM for 4 days. So Y-27632 was a hopeful agent because it releases cell contractions (19) that cause the detachment of cell-sheet. And then the addition of Y-27632 in MFM did not prevent confluent MSC growth in our preliminary experiment (data not shown).

When ROCK, which is Rho-associated protein kinase, was activated within the cell by TGF-β1 (10), actomyosin contractile force was generated (11, 12) and focal adhesions were induced (13, 14). A focal adhesion consists of a large set of proteins, including integrins, submembrane adaptor proteins such as paxillin and vinculin, and

signaling molecules (26). Focal adhesions link the extracellular matrix to bundles of actomyosin, called stress fibers (27). We considered that it is important to regulate focal adhesion and force for production of high-cell-density sheets. As it is difficult to measure cell-generated forces in our system, we monitored paxillin and vinculin included in focal adhesions, which act as "just-in-time" mechanosensing devices, as a reliable indicator for cellular force generation (28). Then MFM including TGF-β1 induced focal adhesions everywhere at the base of cells. The assembly of focal adhesions at the base of cells causes ROCK-dependent contractile force (29–33). It is likely that the force enhanced by multilayered proliferation caused the augmentation of stress in the whole sheet, and this resulted in the detachment of the sheets. Based on the findings obtained by observing paxillin and vinculin, it appears that Y-27632 in MFM inhibited focal adhesion formation, and then cell density and proliferation of the MSC-sheets cultured with MFM/Y were similar to those of the non-CT areas obtained with MFM. We believe that Y-27632, which inhibited focal adhesion formation and the contractile force, maintained cell growth by preventing the detachment of the MSC-sheets.

There are no reports about the effect of ROCK inhibitor Y-27632 on periodontal regeneration. However, Emre *et al.* (21) reported that this reagent is useful for many

applications and safe for cell types. We think that Y-27632 does not disturb periodontal regeneration because we will use it only for *in vitro* proliferation of MSCs. Furthermore, the cells of our sheets cultured with MFM/Y showed similar characteristics to the primary cells and able to differentiate into at least two cell lineages (osteoblastic and adipocytic). Therefore, the cells of our MSC-sheets were considered to be useful in periodontal tissue regeneration.

Recently, there are many experiments using temperature responsive culture methods for the production of cell-sheets (34). However, this method is generally a way to produce a monolayer-sheet and cell-sheets containing many cells were composed of layered monolayer-sheets (35). Gomez et al. (36) *in vivo* reported that temperature responsive culture method was successfully applied to produce periodontal ligament cell-sheets for periodontal regeneration. Nevertheless, they cultured from the third to the fifth passages, differentiated into osteoblasts for 3 weeks, and then layered cell-sheets. We were able to make multilayered cell-sheets remaining multipotencies in about 2 weeks. A further study is planned in which we produce MSC-sheets using our method and temperature responsive culture method, and the effects of those two sheets will be histopathologically compared after transplantation in a rat periodontitis model (37).

Acknowledgements

This work was supported in part by a Grant-in Aid for Scientific Research (C) (22592315) from The Ministry of Education, Culture, Sports, Science and Technology of Japan.

References

(1) Yoshida T, Washio K, Iwata T, Okano T, Ishikawa I. Current status and future development of cell transplantation therapy for periodontal tissue regeneration. *Int J Dent* 2012; **2012**: 307024.

(2) Wilson CE, Dhert WJ, Van Blitterswijk CA, Verbout AJ, De Bruijn JD. Evaluating 3D bone tissue engineered constructs with different seeding densities using the alamarBlue assay and the effect on in vivo bone formation. *J Mater Sci Mater Med* 2002; **13**: 1265-1269.

(3) Winkler T, von Roth P, Matziolis G, Mehta M, Perka C, Duda GN. Dose-response relationship of mesenchymal stem cell transplantation and functional regeneration after severe skeletal muscle injury in rats. *Tissue Eng Part A* 2009; **15**: 487-492.

(4) Shimizu T, Sekine H, Isoi Y, Yamato M, Kikuchi A, Okano T. Long-term survival and growth of pulsatile myocardial tissue grafts engineered by the layering of cardiomyocyte sheets. *Tissue Eng* 2006; **12**: 499-507.

(5) Zhou Y, Chen F, Ho ST, Woodruff MA, Lim TM, Hutmacher DW. Combined marrow stromal cell-sheet techniques and high-strength biodegradable composite scaffolds for engineered functional bone grafts. *Biomaterials* 2007; **28**: 814-824.

(6) Gao Z, Chen F, Zhang J, et al. Vitalisation of tubular coral scaffolds with cell sheets

for regeneration of long bones: a preliminary study in nude mice. *Br J Oral Maxillofac Surg* 2009; **47**: 116-122.

(7) Tsumanuma Y, Iwata T, Washio K, et al. Comparison of different tissue-derived stem cell sheets for periodontal regeneration in a canine 1-wall defect model. *Biomaterials* 2011; **32**: 5819-5825.

(8) Clark RA, McCoy GA, Folkvord JM, McPherson JM. TGF-beta 1 stimulates cultured human fibroblasts to proliferate and produce tissue-like fibroplasia: a fibronectin matrix-dependent event. *J Cell Physiol* 1997; **170**: 69-80.

(9) Tanaka M, Abe T, Hara Y. Roles of focal adhesions and fibronectin-mediated cohesion in proliferation of confluent fibroblasts. *J Cell Physiol* 2009; **219**: 194-201.

(10) Harvey KA, Paranavitana CN, Zaloga GP, Siddiqui RA. Diverse signaling pathways regulate fibroblast differentiation and transformation through Rho kinase activation. *J Cell Physiol* 2007; **211**: 353-363.

(11) Vaughan MB, Howard EW, Tomasek JJ. Transforming growth factor-beta1 promotes the morphological and functional differentiation of the myofibroblast. *Exp Cell Res* 2000; **257**: 180-189.

(12) Brown RA, Sethi KK, Gwanmesia I, Raemdonck D, Eastwood M, Mudera V. Enhanced fibroblast contraction of 3D collagen lattices and integrin expression by

TGF-beta1 and -beta3: mechanoregulatory growth factors? *Exp Cell Res* 2002; **274**: 310-322.

(13) Lee KM, Park J, Kim JH, et al. Reorganization of myosin and focal adhesion proteins in Swiss 3T3 fibroblasts induced by transforming growth factor beta. *Cell Biol Int* 1999; **23**: 507-517.

(14) Dugina V, Fontao L, Chaponnier C, Vasiliev J, Gabbiani G. Focal adhesion features during myofibroblastic differentiation are controlled by intracellular and extracellular factors. *J Cell Sci* 2001; **114**: 3285-3296.

(15) Fukamizu H, Grinnell F. Spatial organization of extracellular matrix and fibroblast activity: effects of serum, transforming growth factor beta, and fibronectin. *Exp Cell Res* 1990; **190**: 276-282.

(16) Ng KW, Tham W, Lim TC, Werner Hutmacher D. Assimilating cell sheets and hybrid scaffolds for dermal tissue engineering. *J Biomed Mater Res A* 2005; **75**: 425-438.

(17) Ishizaki T, Uehata M, Tamechika I, et al. Pharmacological properties of Y-27632, a specific inhibitor of rho-associated kinases. *Mol Pharmacol* 2000; **57**: 976-983.

(18) Davies SP, Reddy H, Caivano M, Cohen P. Specificity and mechanism of action of some commonly used protein kinase inhibitors. *Biochem J* 2000; **351**: 95-105.

(19) Meyer-ter-Vehn T, Sieprath S, Katzenberger B, Gebhardt S, Grehn F, Schlunck G. Contractility as a prerequisite for TGF-beta-induced myofibroblast transdifferentiation in human tenon fibroblasts. *Invest Ophthalmol Vis Sci* 2006; **47**: 4895-4904.

(20) Gauthaman K, Fong CY, Bongso A. Effect of ROCK inhibitor Y-27632 on normal and variant human embryonic stem cells (hESCs) in vitro: its benefits in hESC expansion. *Stem Cell Rev* 2010; **6**: 86-95.

(21) Emre N, Vidal JG, Elia J, et al. The ROCK inhibitor Y-27632 improves recovery of human embryonic stem cells after fluorescence-activated cell sorting with multiple cell surface markers. *PLoS One* 2010; **5**: e12148.

(22) Furuyama A, Mochitate K. Hepatocyte growth factor inhibits the formation of the basement membrane of alveolar epithelial cells in vitro. *Am J Physiol Lung Cell Mol Physiol* 2004; **286**: L939-946.

(23) Abe T, Abe Y, Aida Y, Hara Y, Maeda K. Extracellular matrix regulates induction of alkaline phosphatase expression by ascorbic acid in human fibroblasts. *J Cell Physiol* 2001; **189**: 144-151.

(24) Dominici M, Le Blanc K, Mueller I, et al. Minimal criteria for defining multipotent mesenchymal stromal cells. The International Society for Cellular Therapy position statement. *Cytotherapy* 2006; **8**: 315-317.

(25) Boxall SA, Jones E. Markers for characterization of bone marrow multipotential stromal cells. *Stem Cells Int* 2012; **2012**: 975871.

(26) Wozniak MA, Modzelewska K, Kwong L, Keely PJ. Focal adhesion regulation of cell behavior.*Biochim Biophys Acta* 2004; **1692**: 103-119.

(27) Pellegrin S, Mellor H. Actin stress fibres. *J Cell Sci* 2007; **120**: 3491-3499.

(28) Bershadsky A, Kozlov M, Geiger B. Adhesion-mediated mechanosensitivity: a time to experiment, and a time to theorize. *Curr Opin Cell Biol* 2006; **18**: 472-481.

(29) Totsukawa G, Yamakita Y, Yamashiro S, Hartshorne DJ, Sasaki Y, Matsumura F. Distinct roles of ROCK (Rho-kinase) and MLCK in spatial regulation of MLC phosphorylation for assembly of stress fibers and focal adhesions in 3T3 fibroblasts. *J Cell Biol* 2000; **150**: 797-806.

(30) Totsukawa G, Wu Y, Sasaki Y, et al. Distinct roles of MLCK and ROCK in the regulation of membrane protrusions and focal adhesion dynamics during cell migration of fibroblasts. *J Cell Biol* 2004; **164**: 427-439.

(31) Katoh K, Kano Y, Amano M, Kaibuchi K, Fujiwara K. Stress fiber organization regulated by MLCK and Rho-kinase in cultured human fibroblasts. *Am J Physiol Cell Physiol* 2001; **280**: C1669-1679.

(32) Katoh K, Kano Y, Ookawara S. Rho-kinase dependent organization of stress fibers

and focal adhesions in cultured fibroblasts. *Genes Cells* 2007; **12**: 623-638.

(33) Beningo KA, Hamao K, Dembo M, Wang YL, Hosoya H. Traction forces of fibroblasts are regulated by the Rho-dependent kinase but not by the myosin light chain kinase. *Arch Biochem Biophys* 2006; **456**: 224-231.

(34) Elloumi-Hannachi I, Yamato M, Okano T. Cell sheet engineering: a unique nanotechnology for scaffold-free tissue reconstruction with clinical applications in regenerative medicine. *J Intern Med* 2010;**267**: 54-70.

(35) Sasagawa T, Shimizu T, Sekiya S, et al. Design of prevascularized three-dimensional cell-dense tissues using a cell sheet stacking manipulation technology. *Biomaterials* 2010; **31**: 1646-1654.

(36) Flores MG, Hasegawa M, Yamato M, Takagi R, Okano T, Ishikawa I. Cementum-periodontal ligament complex regeneration using the cell sheet technique. *J Periodontal Res* 2008; **43**: 364-371.

(37) Nakajima K, Abe T, Tanaka M, Hara Y. Periodontal tissue engineering by transplantation of multilayered sheets of phenotypically modified gingival fibroblasts. *J Periodontal Res* 2008; **43**: 681-688.

Figure legends

Fig. 1. Contraction and cell numbers of MSC-sheets. Confluent MSCs were treated with MFM or MFM supplemented with 10 μM Y-27632 (MFM/Y) for 4 days in 24-well plates. (A) Photograph of MSC-sheets. Bar = 5 mm. (B) Proportion of MSC-sheet area to surface area of culture well. *Significantly lower than in MFM/Y ($p < 0.01$). (C) Confluent MSCs were treated with MFM (○) or MFM/Y (●) for 2 or 4 days. The cells were assayed for DNA content. *Significantly higher than MFM on day 4 ($p < 0.01$). Results are the means ± SD of three independent experiments.

Fig. 2. Contraction and proliferation of MSC-sheets. (A–D) Confluent MSCs were treated with MFM or MFM/Y for 4 days in 24-well plates. The cells were labeled with BrdU during the last 20 h of a 4-day incubation. (A–C) Light micrograph of MSC-sheets cultured with MFM. (A) Area of non-contraction (non-CT area). There were a lot of BrdU-labeled cells. (B) Area of contraction (CT area). (C) Detached area. (B,C) CT area and detached area displayed no BrdU-labeled cells. (D) Light micrograph of MSC-sheet's edge cultured with MFM/Y. The nuclei were counterstained with hematoxylin. Dashed line is culture well's wall. BrdU-labeled cells were distributed throughout the cell-sheets. (E) Confocal image of immunofluorescence for cells

cultured with MFM in 4-well Lab-Tek II chamber glass slides. The cell nuclei were stained with TO-PRO-3 iodide (blue). Cell nuclei in the CT areas were elongated and aggregated parallel to the edge. Bar = 100 μm. Similar results were obtained in three independent experiments.

Fig. 3. Multilayer growth of non-CT with MFM and cell-sheet with MFM/Y. (A) Cross-sectional images of MSC-sheet. Confluent MSCs were treated with MFM or MFM/Y for 4 days in 4-well Lab-Tek II chamber glass slides. The cell nuclei were stained with TO-PRO-3 iodide (blue). A z-axis series of confocal images was captured from the base to the top plane of the cells, and the cross-sectional image was obtained by computer processing of stacked images. Upper and lower dashed lines mark the top and base of the cells, respectively. Multilayer growth was observed in both conditions. Similar results were obtained in three independent experiments. Bar = 30 μm. (B,C) Cell density and proliferation of attached MSC-sheets. Confluent MSCs were treated with MFM or MFM/Y for 4 days in 24-well plates. The cells were labeled with BrdU during the last 20 h of a 4-day incubation. Cell density (B) and proliferation (C) of non-CT with MFM, and cell-sheet with MFM/Y. Results are the means ± SD of three independent experiments.

Fig. 4. Confocal images of immunofluorescence for paxillin and cell nuclei. Confluent MSCs were treated with 10% FBS alone, MFM, or MFM/Y for 28 h in 4-well Lab-Tek II chamber glass slides. The cells were stained with mouse mAb against paxillin (green) and TO-PRO-3 iodide (nuclei; blue). Confocal images were obtained at the base plane of the cells. Paxillin assembly in the MFM was localized more than that in the FBS or MFM/Y. There was no difference in the localization of cell nuclei between the three conditions. Similar results were obtained in three independent experiments.
Bar = 100 μm.

Fig. 5. Immunophenotypic profile of cells. Cultured cells of the sheets compared with primary MSCs. Flow cytometry histograms show the expression (shaded) of selected molecules (CD90, CD105, CD146, CD166, CD44, CD19 and CD45) by different cell populations compared with controls (dashed line). Each cell group was positive for the expression of CD90, CD105, CD146, CD166, and CD44, negative for the expression of CD19 and CD45.

Fig. 6. Differentiative potential of cells contained in the sheet. Cells were differentiating to the osteogenic or adipogenic lineage. Light micrograph of ALP staining (A; control, B; osteogenic differentiation). ALP of experimental group was more active than that of control group. Calcium staining of the cultured cells with alizarin red S on day-21 (C). Alizarin red S stainable regions of the cultured cells were detected. Light micrograph of oil red O staining (D; control, E; adipogenic differentiation). The accumulation of lipid vacuoles was observed in the experimental group, but was not in the control.

Bar = 200 μm.

Figure 1.

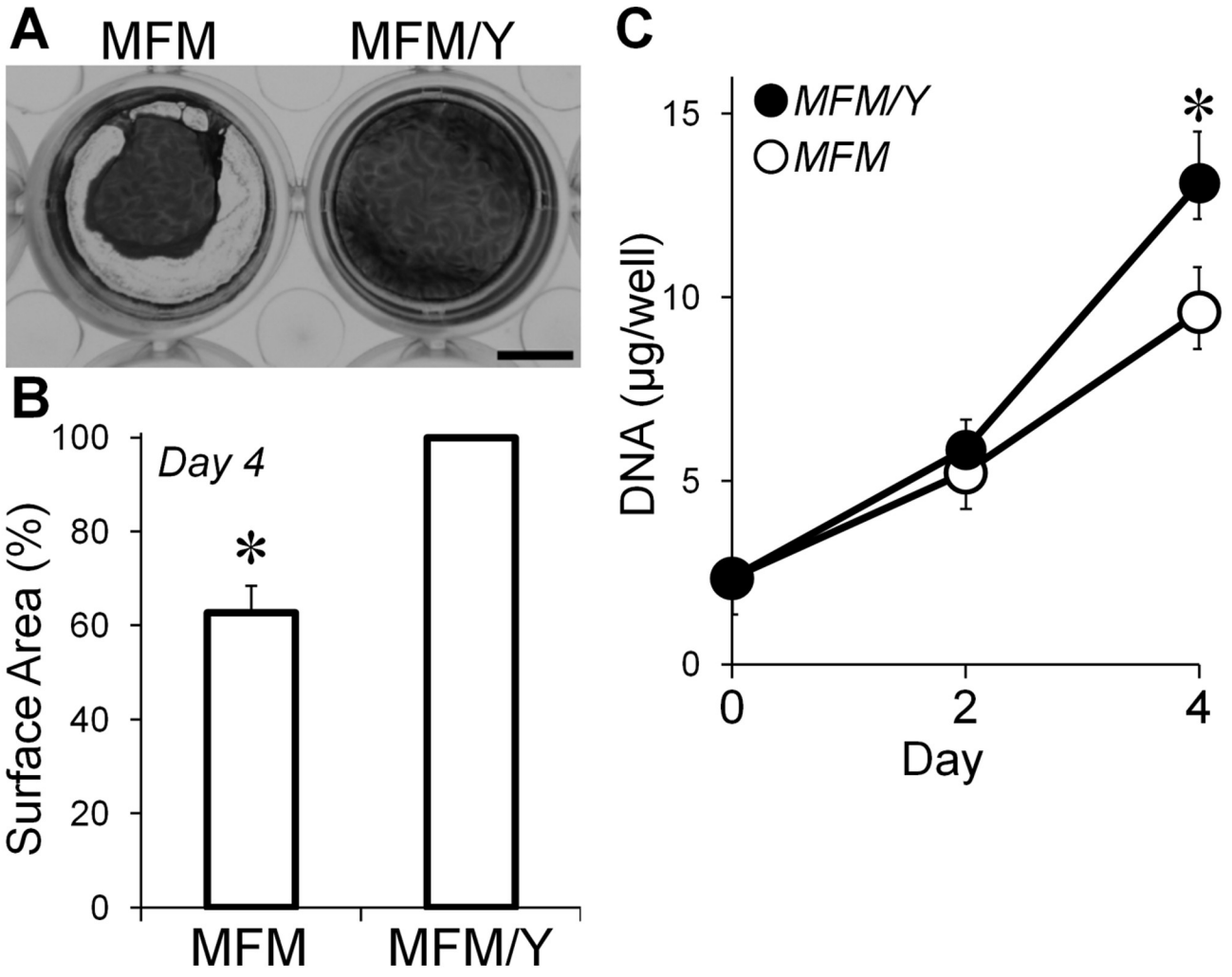
A
MFM
MFM/Y
B
Day 4
Surface Area (%)
100
80
60
40
20
0
*
MFM
MFM/Y
C
MFM/Y
MFM
DNA (µg/well)
15
10
5
0
0
2
4
Day
*

Figure 2.

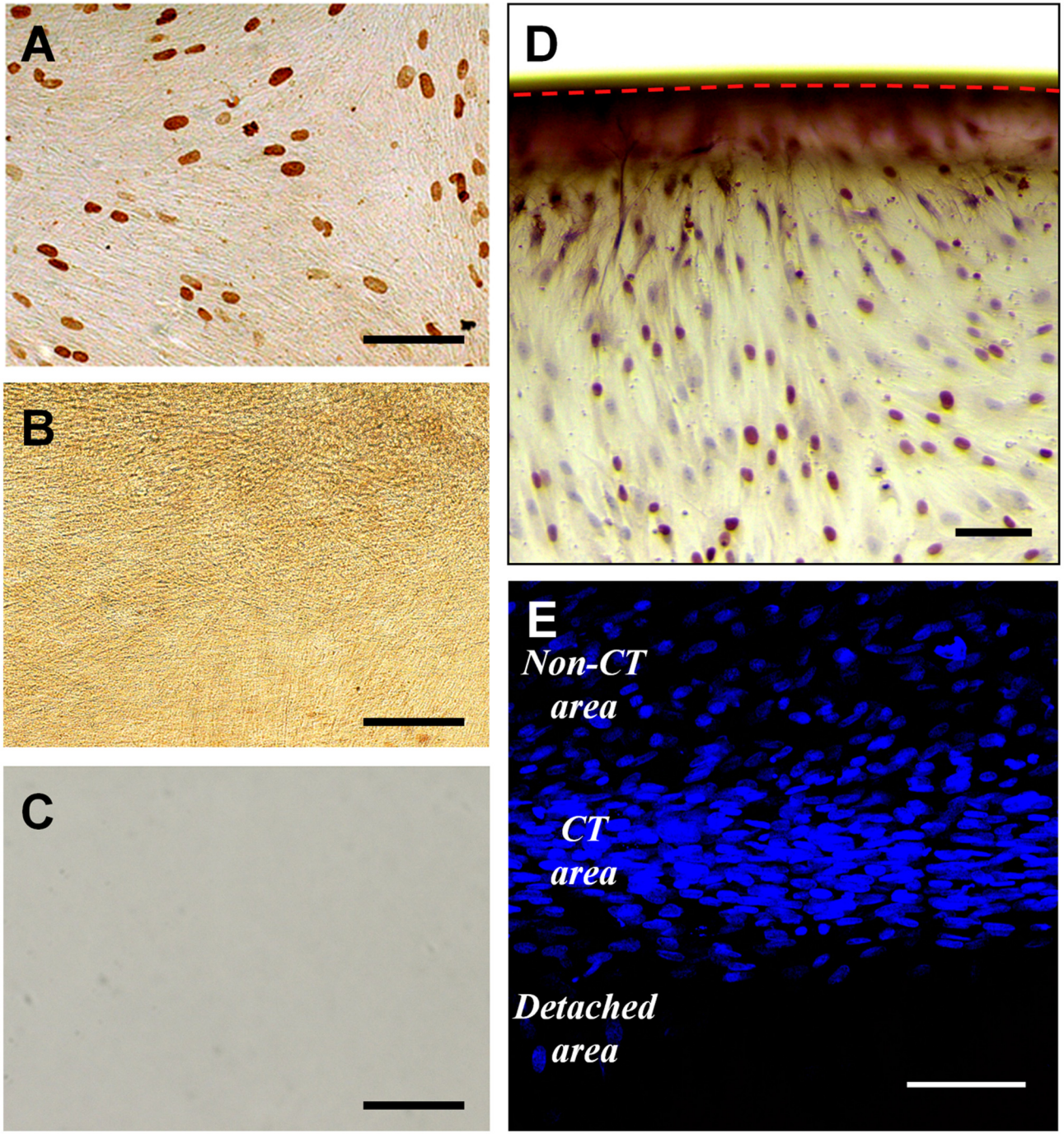

Figure 3.

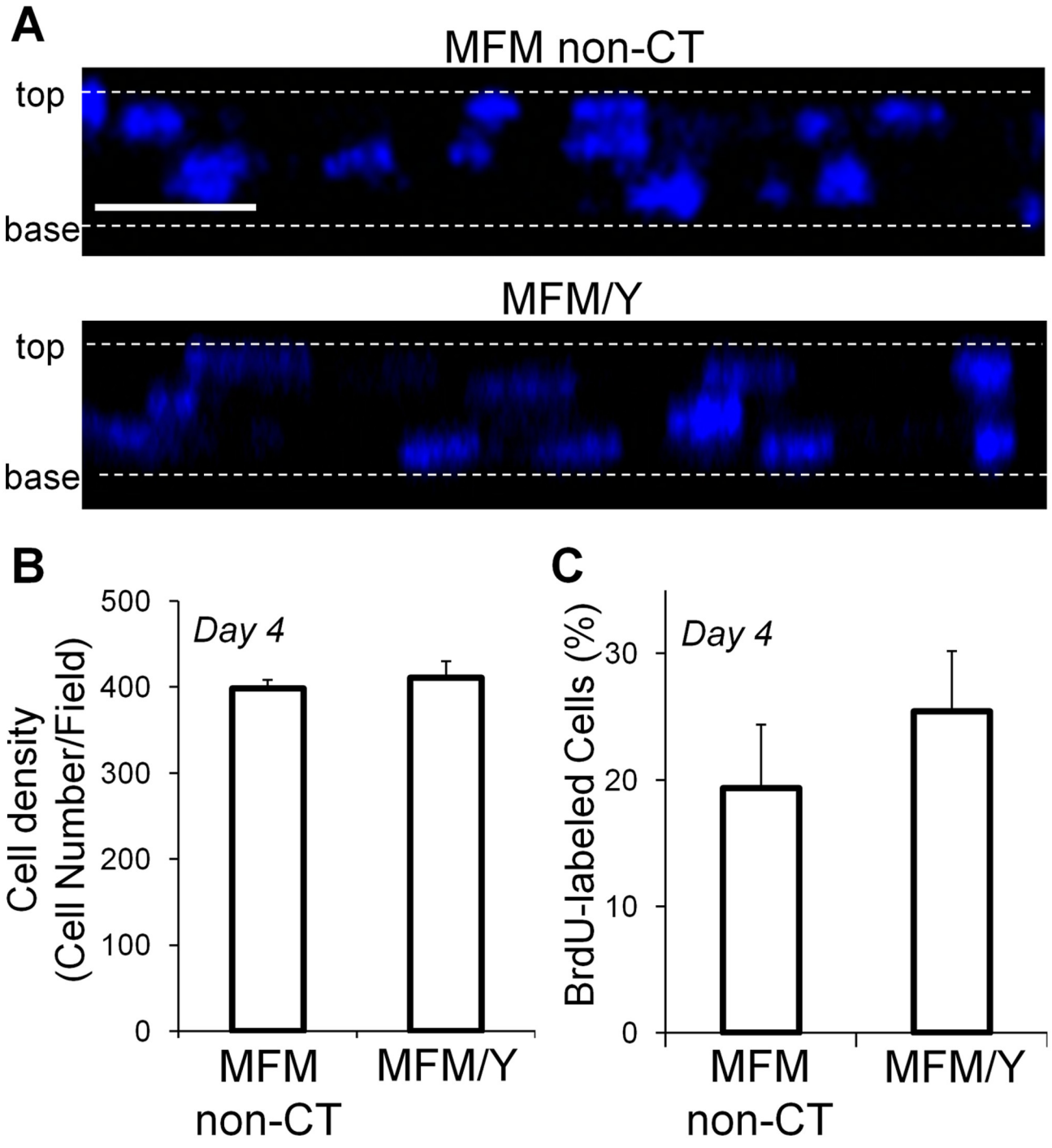
A
MFM non-CT
top
base
MFM/Y
top
base
B
Day 4
Cell density
(Cell Number/Field)
500
400
300
200
100
0
MFM
non-CT
MFM/Y
C
Day 4
BrdU-labeled Cells (%)
30
20
10
0
MFM
non-CT
MFM/Y

Figure 4.

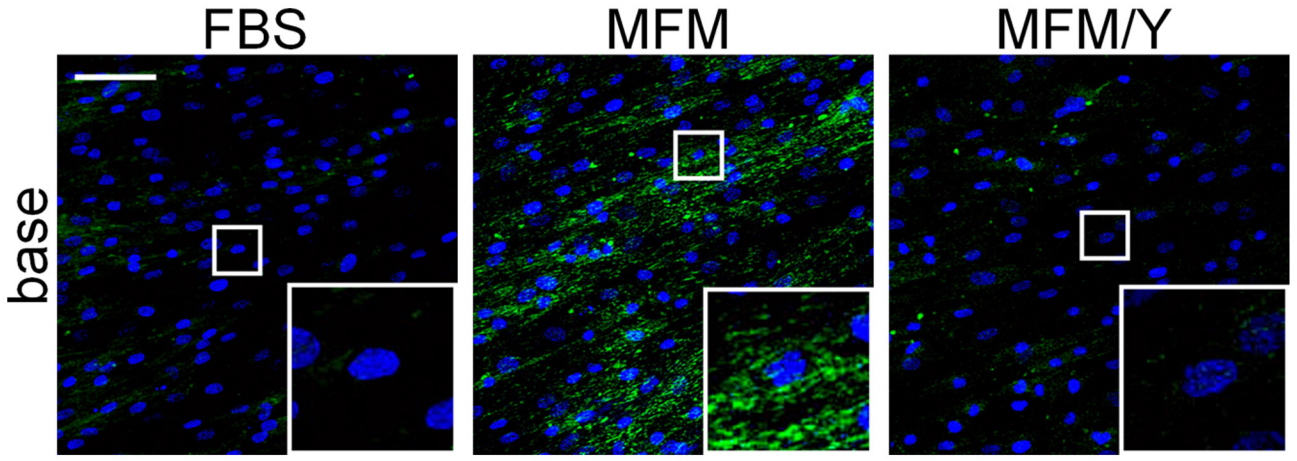

Figure 5.

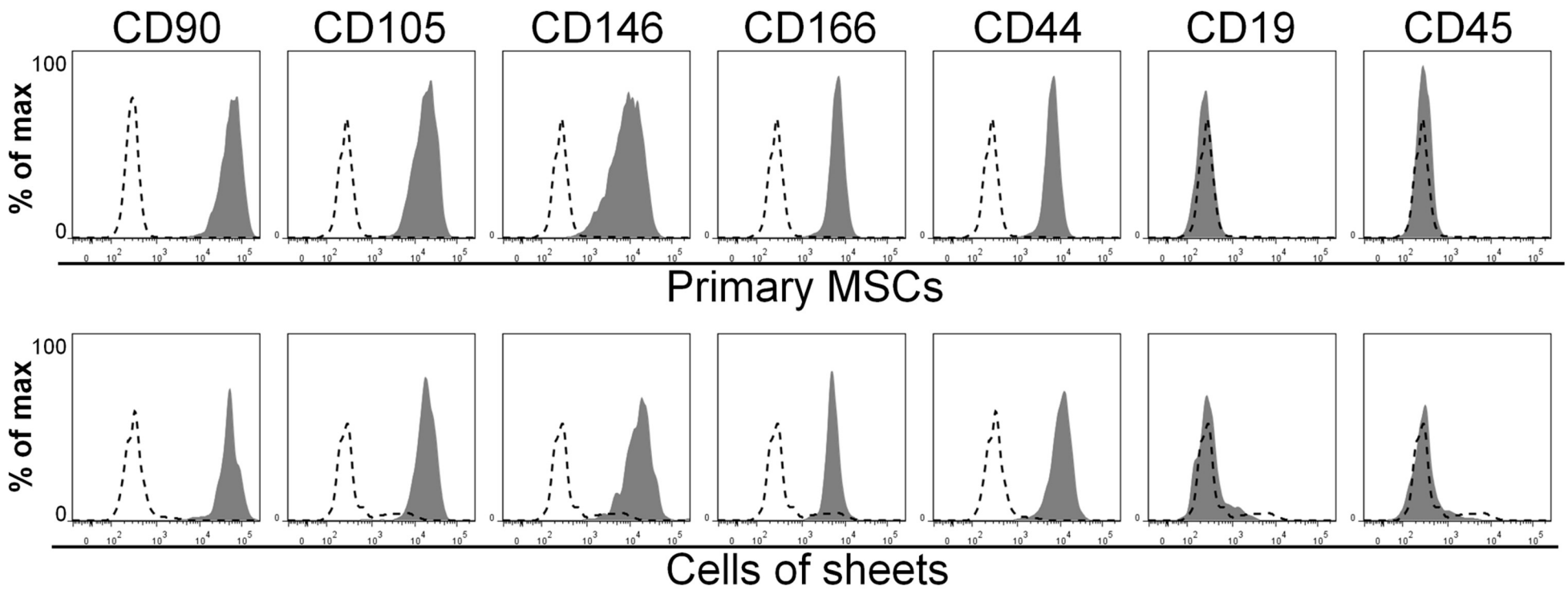
CD90
CD105
CD146
CD166
CD44
CD19
CD45
% of max
100
0
Primary MSCs
Cells of sheets

Figure 6.